

Crystal lattice deformation and the mesophase in poly(ethylene terephthalate) uniaxially drawn by solid-state coextrusion

T. Sun, A. Zhang*, F. M. Li* and Roger S. Portert

Polymer Science and Engineering Department, University of Massachusetts, Amherst, Massachusetts 01003, USA

(Received 31 December 1987; revised 14 May 1988; accepted 23 May 1988)

The development of crystalline and mesophase structure on drawing of poly(ethylene terephthalate) (PET) has been studied. The uniaxial drawing has been done by solid-state coextrusion from 50 to 90°C. The unit-cell parameters of stress-induced crystallites in extrudates have been determined as a function of extrusion draw ratio (*EDR*) up to 4.4 and at an extrusion temperature (*ET*) above T_g , at 70 and 90°C. The higher the *EDR*, the longer the *c*-axis chain direction, the shorter the *a* and *b* axes and the smaller the unit-cell volume. In comparison with the conventional lattice parameters obtained by Bunn and Fisher, the highest elongation of the *c* axis is near 10%. These features imply that the lattice of stress-induced crystallites is far from the closest packing. Coextrudates made below the T_g of PET differ markedly from those made above T_g . Wide-angle X-ray diffraction (WAXD) patterns of PET extruded at 50°C (below T_g) even at high draw ratio exhibit small and/or imperfect crystallites. They appear much as a mesophase. The distance between macromolecular chains ranges from 3.2 to 5.4 Å. The shortest value in the mesophase approaches the interplanar crystal distance of 3.4 Å for the (1 0 0) crystal face, on which the benzene rings lie. The crystalline peak separation of the PET, WAXD curve has been evaluated to obtain absolute crystallinities and the content of mesophase and amorphous phase.

(Keywords: PET; lattice deformation; drawing; coextrusion)

INTRODUCTION

Poly(ethylene terephthalate) (PET) is the most commercially important polyester. There have thus been many studies concerning crystalline and oriented states of PET and over a range of temperatures, draw ratios and deformation rates¹⁻⁶. Intense interest remains concerning the development of high modulus and strength.

A series of films of essentially amorphous PET have been drawn to discrete draw ratios^{7,8} by solid-state extrusion⁹. By extrusion both above and below T_g , a range of morphologies have been developed by variation of draw ratio and temperature. They have been characterized by methods of small-angle light scattering (SALS), cross-polarized microscopy, refractive index and density measurements¹⁰. The development of orientation in crystalline amorphous regions on drawing of comparable samples has been reported¹¹. Relationships between cold crystallization, activation energy for crystallization, extrusion draw temperature and draw ratio have been studied⁸. It is also valuable to understand the crystal lattice features of these uniaxially drawn solid-state extruded films of PET.

Table 1 shows sets of published unit-cell parameters for PET¹²⁻¹⁸; certainly, defects and lattice deformation exist in polymer crystals. Nonetheless, these diverse data are confounding to the belief that there is a discrete set of precise unit-cell parameters for PET. Bosley¹⁹ showed

that crystal lattice displacements could be induced by deformation, heat treatment, cooling rate and by impurities. Fakirov¹⁵ has shown the effect of crystallization temperature and drawing on the *d*-spacing of the crystal lattice of PET. A variation of *d*-spacing has been observed at crystallization temperatures above 148°C. For crystallization at 100°C, *d*-spacing of crystal planes (0 1 0), (1 1 0) and (1 0 0) are longer, corresponding to a crystalline density of 1.484 g cm⁻³. The crystalline density of PET crystallized at 250°C can reach 1.515 g cm⁻³ (see Table 1). It has been assumed that the deviation among reported crystal densities^{12,14,17,18} are due to the variation of chemical composition of PET samples. However, the mole fraction of major impurity, diethylene glycol, in commercial PET ranges only from 0.017 to 0.042, so that it may not significantly influence *d*-spacing. Wakelyn²⁰ has found for a fibre a *d*-spacing of the (1 0 0) and (0 1 0) planes of 3.45 and 5.03 Å respectively, but 3.40 and 5.01 Å respectively for film. They suggested that the Tomasholskii and Markova¹⁴ cell is applicable to PET film, whereas the Daubery, Bunn and Brown¹² cell is applicable to PET fibre. The unit cell for a perfect PET crystal may thus not be suitable as a model for studies of semicrystalline film and fibre, each with their own characteristic strains. Indeed it has been reported that stretching of PET and other polymers causes changes in the *d*-spacing of the (1 0 0) and (0 1 0) planes²¹. A relationship between internal stress and unit-cell parameters in PET fibre has also been proposed²².

Obviously, it is essential to study not only the unit-cell parameters of perfect or equilibrium crystal structures,

* Permanent address: China Textile University, Shanghai, People's Republic of China.

† To whom correspondence should be addressed.

Table 1 Published PET unit-cell parameters

Author	<i>a</i> (Å)	<i>b</i> (Å)	<i>c</i> (Å)	α (deg)	β (deg)	γ (deg)	<i>D</i> (g cm ⁻³)
Bunn ¹²	4.56	5.94	10.75	98.5	118	112	1.455
Astbury ¹³	5.54	4.14	10.86	107.5	112.2	92.23	1.471
Tomasholskii ¹⁴	4.52	5.98	10.77	101	118	111	1.479
Fakirov ¹⁵	4.48	5.85	10.75	99.5	118.4	111.3	1.515
Kinoshita ¹⁶	4.50	5.90	10.76	100.3	118.6	110.8	1.501
Kilian ¹⁷	$d_{(100)}=3.40$ $d_{(010)}=5.02$						1.495
Zahn ¹⁸	$d_{(100)}=3.4$ $d_{(010)}=5.0$						1.501

but also those for the deformed or non-equilibrium crystal structures. The deformed crystal lattices are thus a concern for deformation technologies. In the solid-state coextrusion process of PET, major internal stress is expected. Thus lattice deformation may be present in the extrudates. In this paper, the effects of solid-state extrusion temperature and extrusion draw ratio on lattice deformation of stress-induced PET crystals have been studied. As shown previously, a heat-induced crystallization occurs only above 95°C^{10,11}. Therefore, 90, 70 and 50°C were chosen to initiate stress-induced crystallization.

EXPERIMENTAL

Sample

A PET film with thickness of 25 μm was used. It was virtually amorphous (<2% crystallinity) and isotropic by density and birefringence measurements. The molecular weight, M_n , was about 14 500.

Coextrusion

The PET film was deformed by the split-billet coextrusion technique in an Instron Capillary Rheometer according to a reported procedure^{7,8}.

X-ray diffraction methods

The PET coextrudates were given different exposure times to nickel-filtered Cu K α X-rays to obtain optimally measurable reflections; recorded on film with a Debye-Scherrer camera (evacuated to eliminate air scattering). The patterns were calibrated using the X-ray reflection rings of an added SiO₂ powder. The angular positions of these reflections are determined by using a microprocessor to determine the unit-cell parameters of the PET (triclinic) crystal. The unit-cell parameters of PET were calculated by means of an IBM PC-XT computer.

A Rigaku-3015 X-ray diffractometer was utilized with a wide-range goniometer and Ni filter. The diffraction intensities were recorded at angles $6^\circ \leq 2\theta \leq 36^\circ$. Extrudates were positioned perpendicular to the primary beam. The measured intensities were corrected for air and Compton scattering. To get the crystallinity and the content of mesophase (anisotropic non-crystalline) and isotropic amorphous phases, a method described by Lemanska was adopted²³. The diffraction intensity measured on the equator is summed over the reflection of (010), (1 $\bar{1}$ 0) and (100) planes plus the isotropic and anisotropic diffuse scattering. The intensity on the meridian is considered to be only the isotropic diffuse scattering. A computer program was written for

resolution of overlapping peaks and background on the wide-angle X-ray diffraction (WAXD) curve. In the method proposed below, experimental equatorial scans were fitted to a mathematical model in which crystal peaks were represented as Gaussian and Cauchy functions and the amorphous component as a polynomial

$$I_a(2\theta) = a + b(2\theta) + c(2\theta)^2 + d(2\theta)^3 + e(2\theta)^4 + f(2\theta)^5$$

where *a*, *b*, *c*, *d*, *e* and *f* are adjustable parameters. In this computational procedure, the total intensity at a chosen diffraction angle 2θ was calculated according to the formula:

$$I_{\text{calc}}(2\theta) = I_a(2\theta) + I_{hkl}(2\theta) \quad (1)$$

I_{hkl} denotes the intensity diffracted from the (*h k l*) plane. To eliminate the isotropic component, the meridional scan was subtracted from the amorphous intensities. The mean dimension of the crystallites perpendicular to the (*h k l*) plane were calculated according to the Scherrer formula:

$$L_{hkl} = \frac{K\lambda}{\beta \cos \theta}$$

where *K* is a constant, λ the X-ray wavelength (1.54 Å) and β the breadth at half-maximum intensity of the pure reflection profile (rad).

RESULTS AND DISCUSSION

The X-ray diffraction diagrams of PET coextrudates are shown in Figure 1. For an extrusion draw ratio (*EDR*) above 3.5, three-dimensional order patterns appear for coextrudates prepared at extrusion temperatures (*ET*) of 70 and 90°C. However, the diffraction on the equator is not sharp; diffuse spots are observed on the equator and off-equator for all of the coextrudates. This implies that the crystallites in the coextrudates are imperfect. Coextrudates at 50°C lack the character of three-dimensional diffraction.

Diffraction is concentrated on the equator, with increasing *EDR*. This is characteristic of extreme orientation and low crystallinity. At low *EDR*, the diffraction intensity on the equator for extrudates at 50°C appears stronger than that for extrudates at 70 and 90°C. This implies that the extrudates at 50°C are more anisotropic. This has also been demonstrated by orientation measurements in our earlier work¹¹. The X-ray diffraction patterns show that the pure stress-induced crystallites do not readily form due to limited thermal motion in the solid-state coextrusion of PET, at 50°C ($ET < T_g$). The X-ray pattern (when $ET = 50^\circ\text{C}$) appears

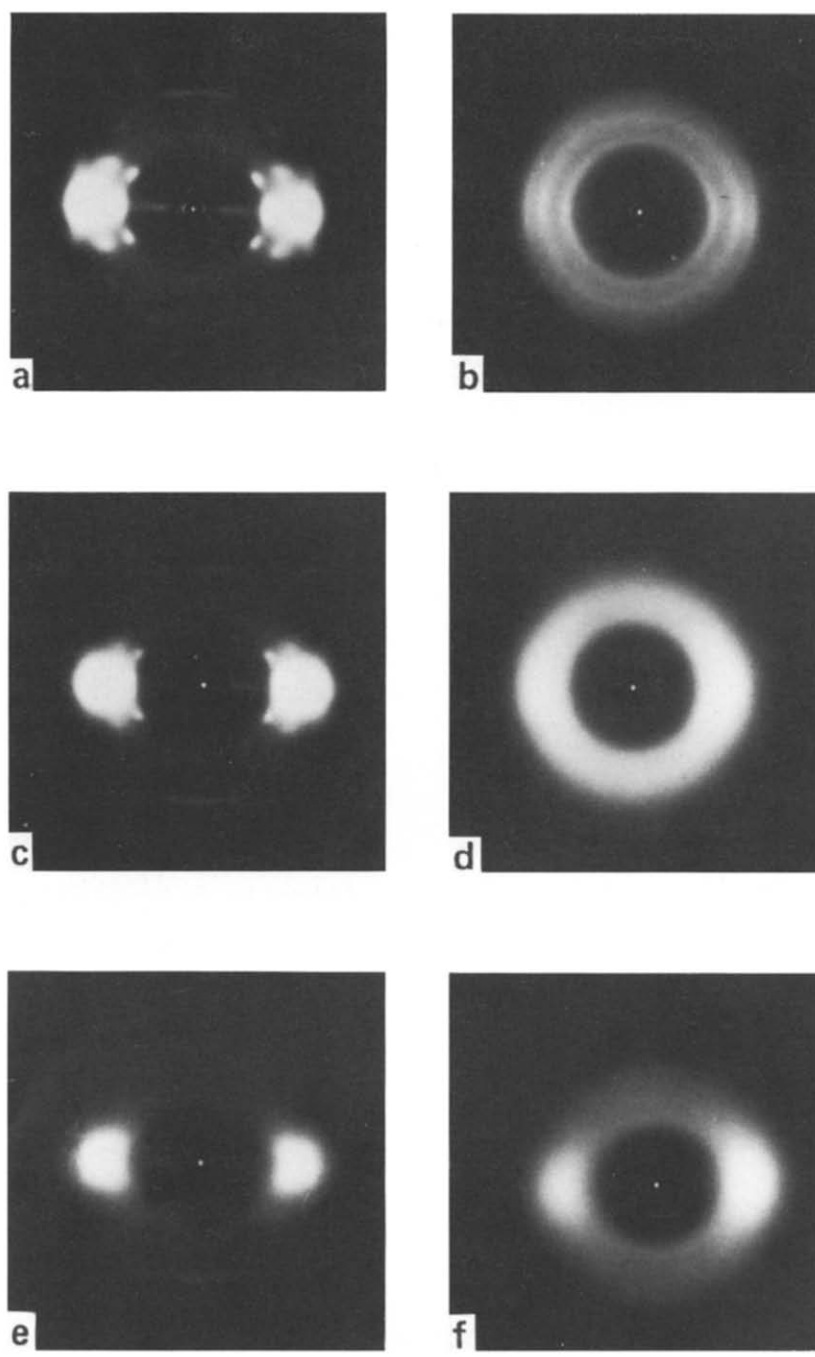


Figure 1 X-ray diffraction patterns of coextrudates drawn at different draw temperatures and ratios: $EDR=4.4$ at (a) 90°C , (c) 70°C and (e) 50°C ; $EDR=2.5$ at (b) 90°C , (d) 70°C and (f) 50°C

more characteristic of an anisotropic non-crystalline phase or a mesophase. There are thus substantial differences in the structures formed on coextrusion below and above the T_g of PET.

The unit-cell parameters determined by X-ray methods for coextrudates at 90 and 70°C are shown in Tables 2 and 3, respectively. The preparations at 90°C show that a larger extrusion draw ratio causes a longer c axis, shorter a and b axes, smaller cell volume and higher density. In comparison with the conventional lattice parameters reported by Bunn¹², the highest elongation of the c axis is near 10%, but the a and b axes show little change. The c -axis elongation results from chain extension on coextrusion drawing. These features imply that the crystal lattice of stress-induced crystallites is far from the closest

packing state. Similarities are found for coextrudates at 70°C , that is, larger extrusion draw ratios induce a longer c , shorter a and b axes and a smaller cell volume. Comparison with the coextrudates at 90°C shows that the higher the draw temperature, the longer the c axis at the same EDR (see Figure 2). In contrast to the crystal lattice of high-speed spun fibres²², the crystal lattice parameters in PET uniaxially drawn by solid-state coextrusion are characterized by a long c axis, implying greater internal stress and a higher modulus.

Both heat-induced and stress-induced crystallization can occur. The differences are due to process history. The stress-induced crystallization causes chain extensions of imperfect crystallites. The dependence of macromolecular crystallization on process history, internal stress,

temperature and time are reflected not only in crystallinity, orientation, crystallite defects and dimension, but also in the parameters of the crystal unit cell.

Figure 1 shows that coextrudates prepared at 50°C do not result in three-dimensional diffraction. The X-ray diffraction distributes continuously along the equator.

Table 2 Unit-cell draw ratio

Extrusion draw ratio	4.4	4.2	3.5
<i>a</i> (Å)	4.37	4.43	4.48
<i>b</i> (Å)	5.87	5.93	5.98
<i>c</i> (Å)	11.57	11.45	11.38
Experimental deviation (Å)	0.03	0.02	0.02
α (deg)	100.1	99.8	99.0
β (deg)	113.4	113.8	114.0
γ (deg)	111.4	113.8	114.0
Volume (Å ³)	234.5	236.5	239.9

Table 3 Unit-cell parameters of PET extruded at 70°C

Extrusion draw ratio	4.4	4.2	3.5
<i>a</i> (Å)	4.42	4.46	4.46
<i>b</i> (Å)	5.93	5.89	6.06
<i>c</i> (Å)	11.43	11.31	11.29
Experimental deviation (Å)	0.04	0.03	0.01
α (deg)	98.6	98.5	99.5
β (deg)	114.6	113.7	114.5
γ (deg)	112.7	112.0	111.9
Volume (Å ³)	233.7	236.3	238.8

The diffraction patterns of these coextrudates are similar, like that of quenched liquid-crystal or mesophase polymer. Diffusion on the equator results from the range of packing. The calculated molecular distances are shown in Table 4. The lower the extrusion draw ratio, the wider the molecular distance distribution. The maximum distances are between 5.04 and 5.4 Å, the minimum distances are between 3.2 and 3.4 Å, with the average probable distance of ~4.0 Å.

It is interesting that the minimum molecular distance approaches the (100) interplanar distance (3.39 Å) of PET crystal. In the PET unit cell, the benzene ring lies approximately on the (100) plane. Because all the atoms of PET lie approximately on the benzene ring plane, the molecular distance reflected by wide-angle X-ray scattering (WAXS) is in fact between benzene rings. By evaluating the diffraction intensity distribution along the equator the molecular distance distribution in mesophase can be calculated.

In 1971 Prevorsek²⁴ first illustrated an intermediate state of order between amorphous and crystalline for PET. This phase has been called 'mesomorphic' or 'anisotropic amorphous'. (In this paper we call it a mesophase or anisotropic non-crystalline phase.) Later, many authors have addressed this question. A method described by Lemanska²³ was adopted here to study the content of mesophase in coextrudates.

All coextrudates with various EDR drawn at 50°C show characteristics of a mesophase. The contents of mesophase and isotropic amorphous phase were calculated by the Lemanska²³ method. The results are seen in Table 5. The mesophase content increases with

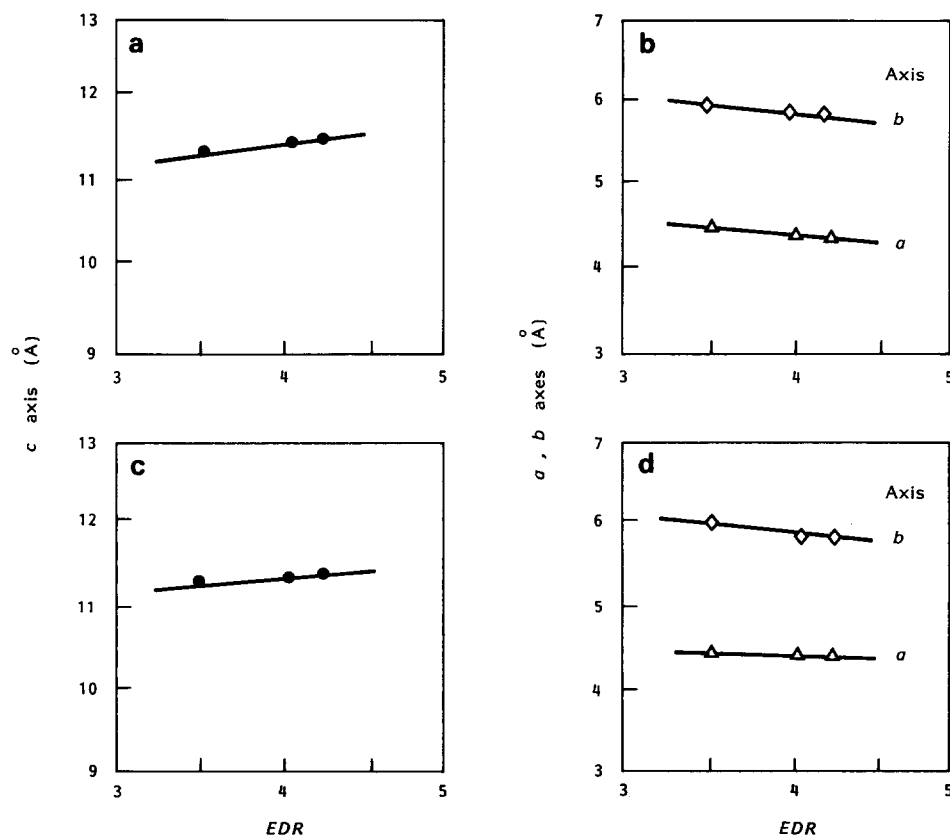


Figure 2 Relationships between draw ratio and unit-cell parameters: (a), (b) drawn at 90°C; (c), (d) drawn at 70°C

EDR, and the isotropic amorphous content decreases. From previous data¹¹, the f_{ave} (average orientation factor calculated from birefringence) and the f_{ad} (amorphous orientation factor calculated from dyeing dichroism) also increase simultaneously. The maximum birefringence of 0.21 (ref. 10) at $EDR=4.4$ approaches a theoretical limit of 0.236 (ref. 25). This implies that solid-state coextrusion at 50°C results in near-perfect orientation along the draw direction. Nonetheless, chains so oriented at 50°C with an EDR of 4.4 do not crystallize effectively. Although PET exhibits mostly minor segment motions below T_g ^{26,27}, stress-induced mesophase is still produced below 50°C. The larger the EDR, the more mesophase is produced. The relationship of f_{ad} , f_{ave} , X_m and X_i with EDR is shown in Figure 3.

Equatorial X-ray diffraction diagrams of coextrudates drawn at 90°C to several EDR are shown in Figure 4. The mesophase content is also calculated and shown in Table 6 by using the Lemanska²³ peak resolution method. The calculations are based on an assumption of three phases: isotropic amorphous, anisotropic non-crystalline (mesophase) and crystalline. The mean dimension of the crystallites calculated according to the Scherrer formula falls into the ranges 27.0–33.3 Å for L_{010} and 23.9–28.0 Å for L_{100} . A comparison may be made with PET fibre from

high-speed spinning with a draw ratio of 1.36 and annealing 4 h at 220°C ($L_{010}=99.7$ Å, $L_{100}=76.1$ Å). The dimension of the crystallites of the coextrudates at 90°C are noted to be smaller, which indicates more imperfection.

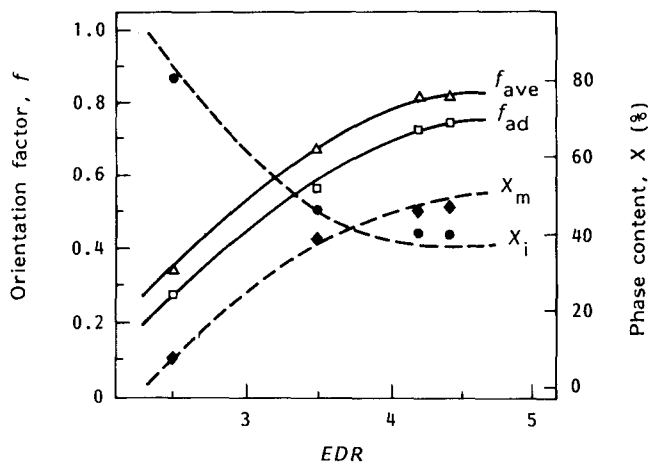


Figure 3 Relationships between f_{ave} , f_{ad} , X_m and X_i of uniaxial coextrudates drawn at 50°C and the draw ratio

Table 4 Molecular distance in PET mesophase from extrusion drawing at 50°C

Extrusion draw ratio	4.4	4.2	3.5
Maximum distance (Å)	5.0	5.4	5.4
Minimum distance (Å)	3.4	3.2	3.2
Distance distribution (Å)	1.6	2.2	2.2
Average distance (Å)	4.0	4.0	4.0

Table 5 Structure parameters^a of uniaxial coextrudates drawn at 50°C

EDR	X_m (%)	X_i (%)	f_{ad} ^b	f_{ave} ^b	D (g cm ⁻³) ^b
4.4	55	45	0.77	0.84	1.359
4.2	48	52	0.74	0.83	1.359
3.5	46	54	0.57	0.69	1.349
2.5	13	87	0.30	0.34	1.347

^a X_m mesophase (anisotropic non-crystalline phase) content

X_i isotropic amorphous phase content

f_{ad} orientation factor obtained from dyeing dichroism measurement

f_{ave} orientation factor obtained from birefringence measurement

^b f_{ad} , f_{ave} and D are borrowed from our previous work¹¹

Table 6 Structure parameters^a of uniaxial coextrudates drawn at 90°C

EDR	X_c (%)	X_m (%)	X_i (%)	f_c ^b	f_{ad} ^b	f_{ave} ^b	D (g cm ⁻³) ^b	L_{010} (Å)	L_{100} (Å)
4.4	65	11	24	0.89	0.58	0.68	1.371	27.0	23.9
4.2	55	16	29	0.86	0.55	0.65	1.365	29.8	24.9
3.5	50	19	31	0.62	0.31	0.42	1.358	33.3	28.0

^a X_c crystallinity

X_m mesophase content

X_i isotropic amorphous phase content

f_c orientation factor obtained from X-ray diffraction

f_{ad} orientation factor obtained from dyeing dichroism measurement

f_{ave} orientation factor obtained from birefringence measurement

L_{hkl} mean dimension of the crystallites perpendicular to (hkl) plane

^b f_c , f_{ave} and D are borrowed from our previous work¹¹

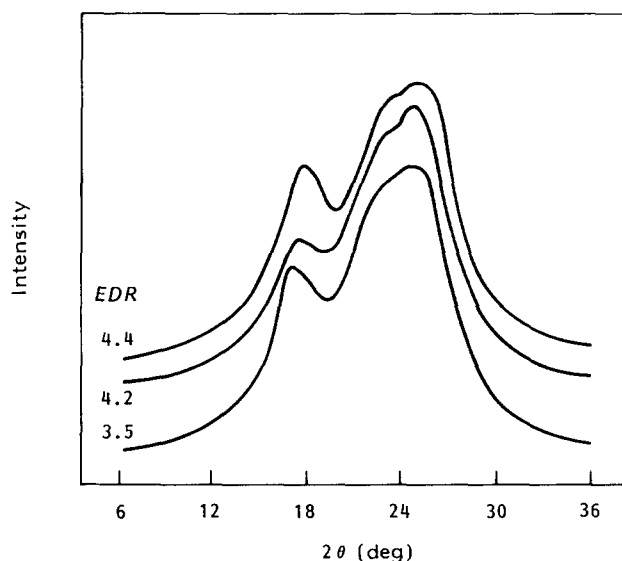


Figure 4 X-ray diffraction diagrams of coextrudates drawn at 90°C

CONCLUSIONS

Coextrudates of PET uniaxially drawn below and above T_g result in major differences in morphology. Above 70°C, the PET exhibits three-dimensional X-ray diffraction of small and imperfect crystallites. All coextrudates made at 50°C exhibit a mesophase. The mesophase content in coextrudates made at 50°C is largest and increases with extrusion draw ratio. The probable intermolecular distance is 4.0 Å. The minimum distance approximates the distance between neighbour planes in crystals on which the atoms of the PET segment lie.

Solid-state extrusion induces PET chain extension which is reflected in unit-cell parameters. The *c*-axis chain direction shows an unusual extension, 11.29–11.57 Å. Comparison with the conventional lattice parameters obtained by Bunn indicates that the highest elongation of the *c* axis is near 10% at the largest extrusion draw ratio.

ACKNOWLEDGEMENT

Appreciation is expressed to the Army Research Office for partial support of this study.

REFERENCES

- 1 Thompson, A. B. in 'Fiber Structure' (Eds. J. W. S. Hearle and R. H. Peters), Butterworth, Washington, DC, 1963
- 2 Thompson, A. B. and Marshall, I. *Proc. R. Soc. Lond. (A)* 1951, **211**, 541
- 3 Thompson, A. B. and Marshall, I. *J. Appl. Chem.* 1954, **4**, 145
- 4 Thompson, A. B. *J. Polym. Sci.* 1959, **34**, 741
- 5 Spruiell, J. E., Macord, D. E. and Beuerlein, R. A. *Trans. Soc. Rheol.* 1971, **16**(3), 535
- 6 Sheldon, R. P. *Polymer* 1963, **4**, 213
- 7 Pereira, J. R. C. and Porter, R. S. *J. Polym. Sci., Polym. Phys. Edn.* 1983, **21**, 1133
- 8 Sun, T., Pereira, J. R. C. and Porter, R. S. *J. Polym. Sci., Polym. Phys. Edn.* 1984, **22**, 1163
- 9 Griswold, P. D., Zachariades, A. E. and Porter, R. S. paper presented at 'Stress-Induced Crystallization Symposium', Midland Macromolecular Institute, Michigan, August 1977
- 10 Sun, T., Kyu, T., Sheng, J., Lefebvre, D., Stein, R. S. and Porter R. S. *J. Appl. Polym. Sci.*, 1985, **30**, 251
- 11 Sun, T., Desper, C. R. and Porter, R. S. *J. Mater. Sci.* 1986, **21**, 803
- 12 Daubery, R. D., Bunn, C. W. and Brown, C. J. *Proc. R. Soc. Lond. (A)* 1954, **226**, 531
- 13 Astbury, W. T. and Brown, C. J. *Nature* 1946, **158**, 871
- 14 Tomasholskii, Y. Y. and Markova, A. S. *Vysomol. Soedin.* 1964, **6**, 27; *Polym. Sci. (USSR)* 1964, **6**, 316
- 15 Fakirov, S., Fisher, E. M. and Schmidt, G. F. *Macromol Chem.* 1975, **176**, 2459
- 16 Kinoshita, Y., Nakamura, R. and Kitano, Y. *Polym. Prepr.* 1979, **20**(1) 454
- 17 Kilian, H. G., Halboth, H. and Jenkel, E. *Polymer* 1960, **166**, 172
- 18 Zahn, H. and Krizikalla, R. *Macromol. Chem.* 1957, **23**, 3
- 19 Bosley, D. E. *J. Appl. Polym. Sci.* 1964, **8**, 1521
- 20 Wakelyn, N. T. *J. Appl. Polym. Sci.* 1983, **28**, 3599
- 21 Sauer, T. H., Wendorff, J. H. and Zimmermann, H. J. *J. Polym. Sci., Polym. Phys. Edn.* 1987, **25**, 2471
- 22 Zhang, A. Q. *Polym. Commun.* 1985, **3**, 216
- 23 Lemanska, G. and Narebska, A. *J. Polym. Sci., Polym. Phys. Edn.* 1980, **18**, 917
- 24 Prevorsek, D. C. *J. Polym. Sci.* 1971, **32**, 343
- 25 Wlochowicz, A., Rabiej, S. and Janicki, J. *J. Appl. Polym. Sci.* 1983, **28**, 1335
- 26 Mayban, K. G., James, W. J. and Bosch, W. J. *J. Appl. Polym. Sci.*, 1965, **9**, 3605
- 27 Ito, E., Yamamoto, K., Kobayashi, Y. and Hatakayama, T. *Polymer* 1978, **19**, 39